

FLUORESCENCE CHARACTERISTICS OF THE UPPER WATER LAYER OF THE ARCTIC SEAS BASED ON LIDAR, SPECTROPHOTOMETRIC, AND OPTICAL METHODS

*Violetta Drozdowska¹, Waldemar Walczowski², Ryszard Hapter¹, Joanna Stoń¹,
Miroslaw Irczuk², Tymon Zieliński² and Jacek Piskozub²*

1. Institute of Oceanology, PAS, Marine Physics Department, Sopot, Poland;
{drozd/hapter/aston}@iopan.gda.pl
2. Institute of Oceanology, PAS, Marine Hydrodynamics Department, Sopot, Poland;
{walczowsk/irczuk/tymon/piskozub}@iopan.gda.pl

ABSTRACT

Lidar and optical data combined with the ground-truth measurements from a great number of stations spread across Greenland and the Norwegian Seas yield a large database partly presented and analysed herein. The intensities of the emission bands of the lidar-induced water spectrum, the diffuse attenuation coefficients, and the surface concentration of chlorophyll *a* are used to describe the spatial distribution of the fluorescent molecules in the upper water layer. The characteristics of vertical profiles of the chlorophyll *a* content are given as well.

A comparison between lidar estimations of chlorophyll *a* content and extracted chlorophyll *a* from water sampling, and hydro-physical parameters of water is presented.

Keywords: Arctic Seas, chlorophyll *a* distribution, fluorescence lidar

INTRODUCTION

The Greenland and Norwegian Seas represent a very interesting region that is the mixing area of salty and warm water of Spitsbergen current with cool and fresh glacial water (1). Therefore, the investigations of the phytoplankton biomass density changes in the surface water layer, influenced by factors such as salinity and temperature of water and water circulation, allow the patchiness of fresh and ocean water inflow to be investigated (2,3).

The data were collected in one expedition. The cruise, lasting one month, took place in the arctic summer (mid June – mid July 2002) and was part of the Institute of Oceanology AREX program. The measurement stations are presented in Figure 1.

The intensities of the fluorescence bands occurring in the lidar-induced water spectra are analysed based on the water diffuse attenuation coefficients K_d (recorded in several spectral bands) and the surface concentration of the chlorophyll *a*, C_a , (at 0 m level) (4, 5). The interpretation of the above results yields the horizontal distribution of chlorophyll *a* content as well as the vertical profiles of the chlorophyll *a* density in the upper water layer.

METHODS

Temperature, salinity, and density (CTD) measurements were made at all stations. The temperature and salinity profiles were obtained with records made down to the bottom using a Sea-Bird 9/11 CTD probe. Readings were averaged every 1 and 5 dbars. Figure 2 demonstrates the spatial distribution of the temperature and salinity at a depth of 10 m. Figure 5 shows the current vectors calculated on the base of CTD monitoring.

The lidar measurement stations occurred less frequently than the CTD stations and were carried out simultaneously with optical and ground-truth measurements.

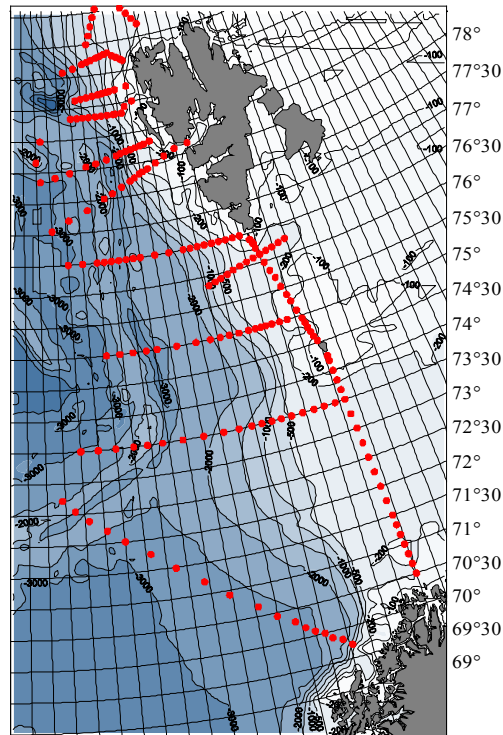


Figure 1: AREX 2002 station map.

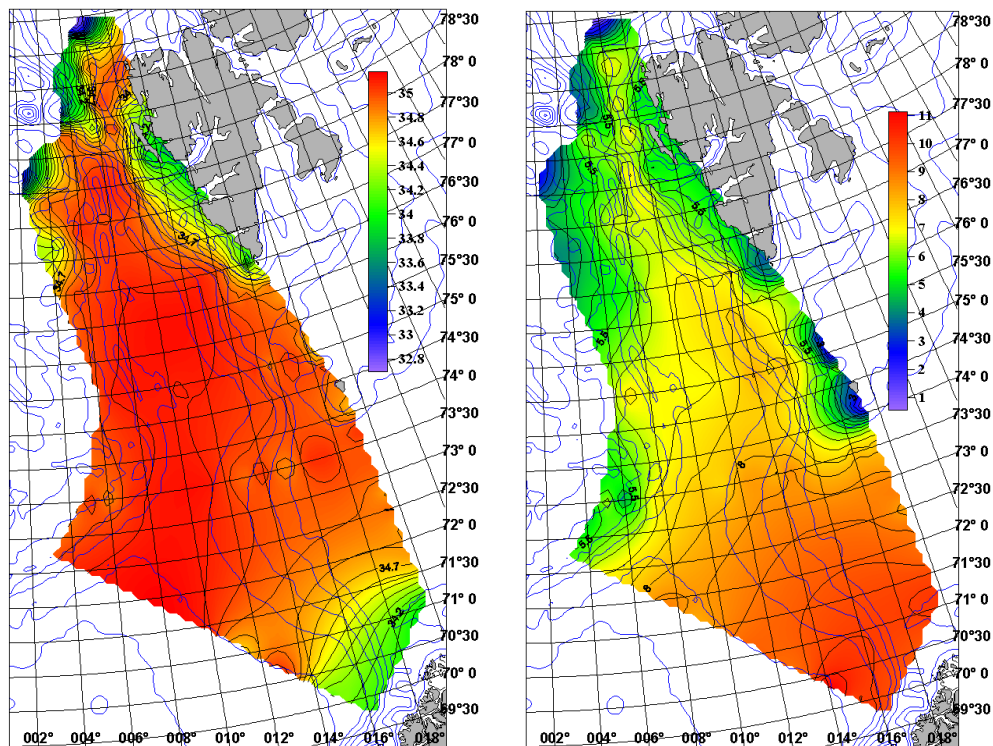


Figure 2: Salinity (left) and temperature ($^{\circ}\text{C}$) (right) in the layer 0-10 m

The FLS-12 lidar was fixed on board of R/V *Oceania*. The distance x_0 between the telescope and water surface was about 6 m. The lidar-induced return signal was accumulated and averaged from about 50 seawater fluorescence spectra with a long time-gate allowing the fluorescence emitted from the uppermost water column to be recorded. The return signals, excited at 440 nm, are registered in a continuous spectral range from 360 to 760 nm (with 0.8 nm spectral resolution). The fluorescence factors of the fluorescent substances $F(\lambda_{ex})$ obtained as the ratio of the integrals of

the fluorescence and water Raman scattering band intensities give information about the intensity of the fluorescence emission depending on the chlorophyll *a* concentrations contained in a water column (6).

The optical data were collected using a multi-channel spectroradiometer, designed in IO PAS, equipped with sensors to measure the down-welling irradiance of the sea surface and the water-leaving radiance to depths of several ten-meters in several spectral bands (with a half-width of 10 nm). The in-water optical data were obtained from down casts filtered and binned into 1 m intervals.

Surface water samples were taken just after the optical sensors were deployed. The samples were filtered onto GF/F glass fibre filters and kept in liquid nitrogen until they were analysed in the laboratory. The chlorophyll *a* (chl *a*) concentration was estimated spectrophotometrically according to Jeffrey & Humphrey (7). These chl *a* data were used for normalizing the fluorescence spectra intensity.

The inverse problem of lidar measurement

The results presented herein, formulated as a lidar inverse problem, are based on the lidar-induced seawater spectra and the diffusion attenuation coefficient K_d of the downward irradiance E_d (443, 510, 589 and 670 nm) and the chl *a* measurements. The intensity of the lidar return signal is described by the lidar equation:

$$dI^{theo} = d\Phi_{fl} A \frac{I_o}{x^2} e^{-(x-x_o)(K_{d,l}+K_{d,fl})}, \quad (1)$$

where A is a constant describing the environmental and lidar system coefficients, $x - x_o$ is the water depth where the signal dI has been excited, indices l and fl describe the wavelengths of the laser and fluorescence light, respectively. The term $d\Phi_{fl}$ describes the efficiency of the fluorescence process, given by the formula:

$$d\Phi_{fl} = dN_{fl} \cdot \sigma_{fl} = n_{fl} \cdot \sigma_{fl} \cdot S \cdot dx, \quad (2)$$

where dN_{fl} is the number of the fluorescent molecules in a defined water volume $dV = S \cdot dx$, n_{fl} is the concentration and σ_{fl} the fluorescence cross-section of the investigated molecules. Finally, inserting $d\Phi_{fl}$ given by formula 2) into formula 1) one obtains:

$$dI^{theo}(x) = A \cdot \frac{n_{fl} \sigma_{fl} dx}{x^2} I_o \cdot e^{-(x-x_o)(K_{d,l}+K_{d,fl})}. \quad (3)$$

The fluorescence intensity of the water column between surface and depth z can be calculated as the following integral:

$$I_z^{theo}(z) = \int_{x_o}^{x_o+z} dI^{theo} = \int_{x_o}^{x_o+z} I^{theo}(x) dx = n_{fl} A I_o \int_{x_o}^{x_o+z} \frac{1}{(x_o+z)^2} e^{-(x-x_o)(K_{d,l}+K_{d,fl})} dx, \quad (4)$$

For a comparison of the surface concentration of chl *a* (C_a) with the concentration n_{fl} of the fluorescent molecule, we assume $z = 0.5$ m. Then, because $z \ll x_o$ it can be assumed that

$$\left(\frac{1}{x_o+z} \right)^2 \cong \left(\frac{1}{x_o} \right)^2 = const$$

in the integration interval of equation 4). Taking this factor out of the integral the intensity of the return spectrum can be calculated as:

$$I_z = I^{theo}(z) = n_{fl,z} \sigma_{fl,z} \frac{A I_o}{x_o^2} \frac{1}{K_{d,l} + K_{d,fl}} \left(1 - e^{-z(K_{d,l}+K_{d,fl})} \right). \quad (5)$$

Dividing the total fluorescence emission signal of the layer of the thickness z by the water Raman signal of the same layer one obtains an expression that depends only on the attenuation coefficients K_d and the fluorescence efficiency of the fluorescent substance:

$$F^{theo}(\lambda_{ex}) = \frac{I_{fl,z}}{I_{R,z}} = \frac{1 - e^{-z(K_{d,l} + K_{d,fl})}}{1 - e^{-z(K_{d,l} + K_{d,R})}} \cdot \frac{K_{d,l} + K_{d,R}}{K_{d,l} + K_{d,fl}} \cdot \frac{n_{fl,z}\sigma_{fl}}{n_{R,z}\sigma_R} \equiv C \cdot \frac{K_{d,l} + K_{d,R}}{K_{d,l} + K_{d,fl}} \cdot n_{fl,z} \cdot \sigma_{fl,z}, \quad (6)$$

where $C = const.$

On the other hand, the lidar data are exploited to calculate the values of the fluorescence factor:

$$F(\lambda_{ex} = 440nm) = \frac{I_{fl}^{exp}}{I_R^{exp}} = \frac{\int_0^{\infty} I_{fl}(x)dx}{\int_0^{\infty} I_R(x)dx}, \quad (7)$$

where I_{fl}^{exp} and I_R^{exp} are the spectral signal intensities. From Figure 3 it can be justified that 30 m is the maximum integration depth. Therefore, the registered spectra contain information about the average abundance of phytoplankton in the water column.

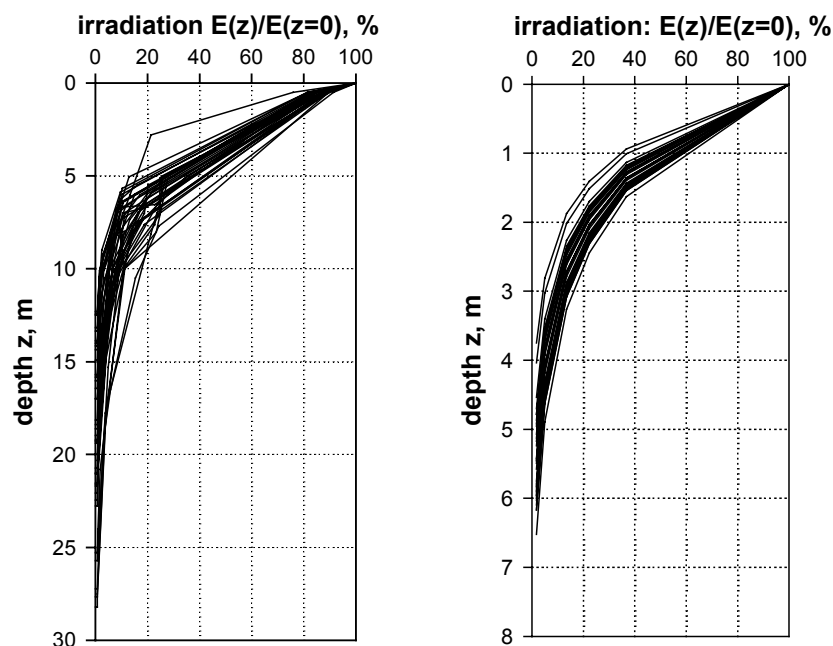


Figure 3: The penetration depths of lidar-induced water Raman scattering (left) and fluorescence (right).

Applying various time-gate delays yields values of the fluorescence factor $F(\lambda_{ex})_z$ for different depths, z , of the water column.

$$F(\lambda_{ex} = 440nm)_z = \frac{I_{fl}^{exp}(z)}{I_R^{exp}(z)} = \frac{\int_{x_0}^{x_0+z} I_{fl}(x)dx}{\int_{x_0}^{x_0+z} I_R(x)dx}. \quad (8)$$

The factor $F(\lambda_{ex})_z$ depends only on the attenuation properties K_d of water if the water column within the lidar penetration depth is well mixed. Then $F(\lambda_{ex})_z$ changes proportionally to $n_{fl,z} \cdot \sigma_{fl,z}$ (equation 6). Any deviations from this proportionality mark the varying abundance of phytoplankton or fluorescence properties of chl a in the column with depth z . Therefore, we define the factor χ_z :

$$\chi_z = \frac{n_{fl,z} \sigma_{fl,z}}{C_a} \tag{9}$$

Assuming that the fluorescence cross-section of chl a is constant, any disproportional changes in values of equation 9) indicate an inhomogeneous distribution of chl a density in the water column.

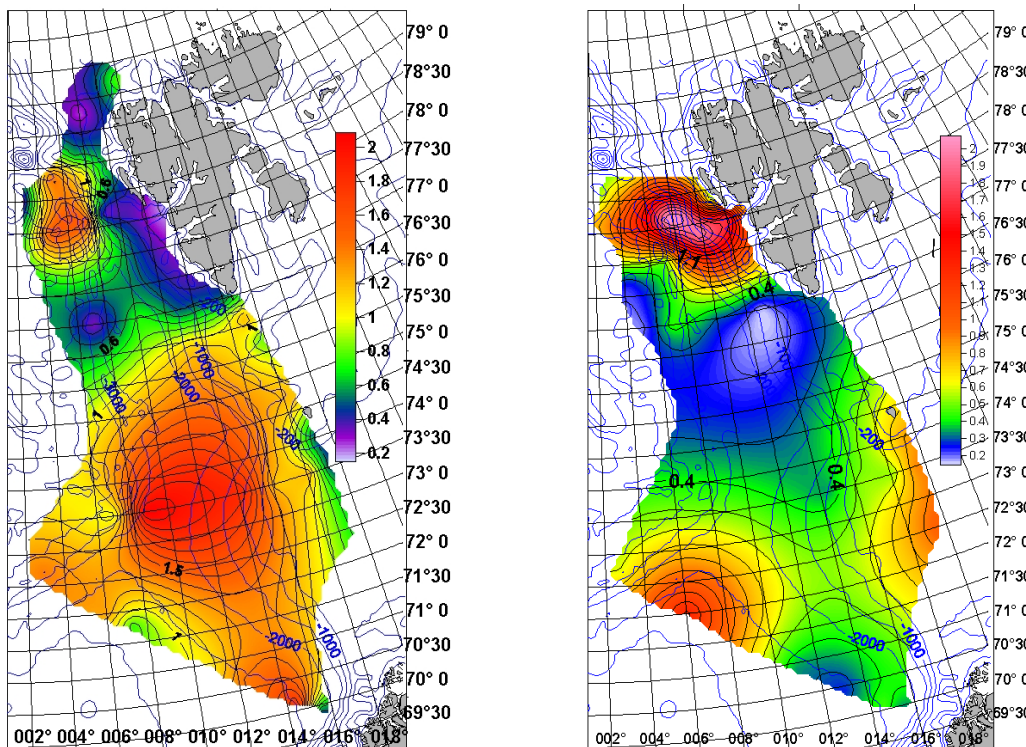


Figure 4: Distribution of surface concentration of chlorophyll a, C_a , mg/l (left) and of the fluorescence factor $F(\lambda_{ex_z} = 440nm)_z$ in relative units normalized to maximal value of C_a (right).

Thus the map of the fluorescence factor, $F(\lambda_{ex})_z$ (Figure 4), of chl a gives information about the phytoplankton abundance in the upper water layer. Additionally, the fluorescence factor $F(\lambda_{ex})_z$ combined with K_d and C_a provides vertical profiles χ_z of the chl a density in the upper water layer (Figure 5).

RESULTS

Surface concentrations of chl a ranging from 0.2 to 2.2 mg/l, are presented in Figure 4.

The lidar data, calculated in relative units and normalized to the maximal value of C_a , therefore vary within the same limits as the surface concentration C_a (Figure 4). The lowest values of the surface concentration C_a occur around the western and southern Spitsbergen coasts, while the fluorescence factor $F(\lambda_{ex})_z$ reaches its highest values there.

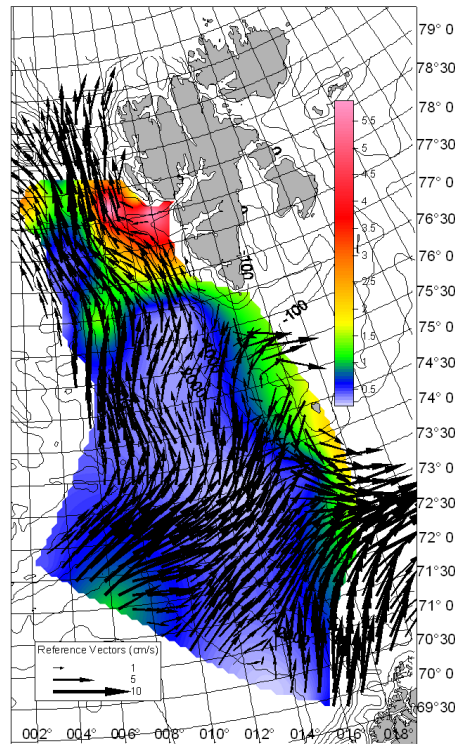


Figure 5: The disproportion, χ_z , between lidar results and data from water sampling; the baroclinic currents vector at 50 m depth, reference level is 800 m.

The central region of the studied area, between 8°–15° E longitude and 71°–76°N latitude, includes water masses characterised simultaneously by high surface concentration C_a (0.9–2.1 mg/l), Figure 4 (left) and medium values of chl a $F(\lambda_{ex})_z$ (0.2–0.5 rel.u.), Figure 4 (right). Moreover, temperature and salinity reach the highest values (above 5.5°C and S=34.7, respectively) in the upper layer, 0–10 m, Figure 2. This area includes well-mixed water masses described by a low value of the factor χ_z and is characterised by high values of the current vector of the water circulation, Figure 5.

The opposite situation, i.e. $F(\lambda_{ex})_z$ of chl a is higher (0.8–2.2 rel. u.) than the surface concentration C_a (0.2–0.8 mg/l), was found around the southern and western coasts of Spitsbergen and around Bear Island, Figure 4. The values of the chl a fluorescence factor $F(\lambda_{ex})_z$ are by far higher than the surface C_a values indicate. Thus, the abundance of phytoplankton in the water column is very high, Figure 5. Low temperature (beneath 5.5°C) and low salinity (32.7–34.7) as well as their distinct gradients characterise these regions in the 0–10 m upper layer, Figure 2, characterise the west Spitsbergen Current, going from north-eastern direction and carrying large inflows of fresh water, Figure 5.

CONCLUSIONS

The study region constitutes an area that is very characteristic of movements and mixing water masses. The results, Figure 5, present warm Atlantic waters mixed with cold, nutrient-rich waters from Arctic and melting glacial. Owing to remarkable dynamic activity (with surface and under surface currents and whirls) there arise differences in the hydro-physical and biological parameters, which become manifest in the manifold abundance of phytoplankton.

The central area of studied seas is described by rather high values of the surface concentration C_a and lower values of the fluorescence factor $F(\lambda_{ex})_z$ of chl *a* ($\chi_z < 1$) (Figure 5). Thus, the biological life of phytoplankton is contained rather in the same surface water layer.

The regions located around the southwestern coasts of Spitsbergen and the Bear Island, abound with rich biological life. Despite the minimal values of the surface concentration C_a , the phytoplankton contained in all water columns gave a strong fluorescence signal of chl *a*.

REFERENCES

- 1 Piechura J & W Walczowski, 1996. Interannual variability in the hydrophysical fields of the Norwegian-Barents Seas confluence zone Oceanologia, 38(1), 81-99
- 2 Markowski D & J Wiktor, 1998. Phytoplankton and water masses in the European subarctic Polar Front. Oceanologia, 40(1): 51-65
- 3 Weslawski J M, J Wiktor & S Kwasniewski, 1991. R/V "Oceania" survey on the Norwegian and Greenland Seas in 1987-1989. Plankton species composition. SIMO, 58: 187-202
- 4 Babichenko S, S Kaitala, A Leeben, L Poryvkina & J Seppala, 1999. Phytoplankton pigments and dissolved organic matter distribution in the Gulf of Riga. Journal of Marine Systems, 23: 69-82
- 5 Hoge F E & R N Swift, 1981. Airborne simultaneous spectroscopic detection of laser-induced water Raman backscatter and fluorescence of chlorophyll *a* and other naturally occurring pigments. Applied Optics 20: 3197-1205
- 6 Drozdowska V, S Babichenko & A Lisin, 2002. Natural water fluorescence characteristics based on lidar investigations of surface water layer polluted by an oil film; the Baltic cruise – May 2000, Oceanologia, 44 (3), 339-354.
- 7 Jeffrey S W & G F Humphrey, 1975. New spectrophotometric equations for determining chlorophylls *a*, *b*, *c*1 and *c*2 in higher plants, algae and natural phytoplankton, Biochemie und Physiologie der Pflanzen, 167: 191-194